

Decentralized Real-Time Energy Management for A Reconfigurable Multiple-Source Energy System

He Yin, *Member, IEEE*, Chen Zhao, Chengbin Ma, *Senior Member, IEEE*

Abstract—This paper discusses decentralized real-time energy management for multiple-source hybrid energy systems (HESs) that adapts to the sudden change in system configuration such as due to failure of certain devices. An engine-generator/battery/ultracapacitor (UC) HES is chosen as a case study facilitating the following theoretical discussion. The energy management problem is first modeled as a non-cooperative game, in which the different preferences of the energy sources (engine-generator, battery pack, and UC pack) in actual operation are quantified through their individual utility functions. The Nash equilibrium is iteratively reached at each control instant via a learning algorithm. Under the game theory-based control, each source or player tends to maximize its own preference. However, its satisfaction level also depends on decisions of others. This real-time interaction in decision making provides the proposed energy management a capability to autonomously adapt to the reconfigured HES. A tuning procedure of weight coefficients in the utility functions also helps to further improve the adaptiveness of the decentralized energy management. Both the simulation and real-time implementation show that the game theory-based energy management strategy has a comparable performance to the classical centralized benchmarking strategy. Meanwhile, the decentralized strategy demonstrates an obvious flexibility handling the cases when the configuration of the HES varies both statically and dynamically.

Index Terms—Hybrid energy system, multiple sources, decentralized control, game theory, reconfiguration.

NOMENCLATURE

g, G	Engine-generator
b, B	Battery pack
c, C	Ultracapacitor pack
l	Load
u_x	Utility functions ($x = g, b, c, l$)
$u_{x,l}$	Final form of utility functions ($x = g, b, c$)
i_x	Output currents ($x = g, b, c$)
i_l^*	Load command

a_x, b_x, c_x	Coefficients in u_x ($x = g, b, c$)
$I_{g,opt}$	Engine generator optimal output current
$I_{b,ave}$	Battery average output current
$I_{b,l}$	Battery last output current
$I_{c,fit}$	Ultracapacitor target charge/discharge current
ω_x	Weights relating to sources in $u_{x,l}$ ($x = g, b, c$)
$\omega_{l,x}$	Weights relating to load in $u_{x,l}$ ($x = g, b, c$)
ε	Threshold for reaching Nash equilibrium
Θ_x	Threshold for w_x adaptive tuning ($x = g, b, c$)
$C_{g,ave}$	Average engine-generator fuel consumption
$Q_{b,loss}$	Battery capacity loss
$SOC_{c,ave}$	Average UC pack SOC
$I_{dif,ave}$	Average load demand and current difference
t_{sim}	Simulation time

I. INTRODUCTION

DUE to the complementary features of various energy storage and generation devices, hybrid energy systems (HESs), i.e., the combination of heterogenous energy sources, have been intensively investigated in recent years. These systems have wide applications in electric vehicles (EVs), smart houses, microgrids, and smart grids, etc. A typical HES usually consists of multiple major energy sources (battery, fuel cell, photovoltaic panel, wind turbine, and engine generator, etc.) and also assistive ones such as ultracapacitor (UC) and flywheel [1]. For example, the basic concept of a battery/UC HES is to use UCs, which have a high power density, as a buffer to improve the performance of the overall system in terms of efficiency, dynamic response, and protection of battery [2]. A comprehensive review on UCs, in terms of their control and management aspect, can be found in [3], which summarizes the progresses on the modeling, state estimation, and applications of UCs. It is especially interesting to note that fractional-order calculus has been applied to improve the accuracy in UC modeling and state of charge (SOC) estimation [4]. The hybridization of batteries and UCs also helps to avoid an oversized battery pack when meeting a dynamic load demand. Further combination with other types of energy storage devices and generators has been proved to be a feasible solution to better satisfy the energy and power requirements in different applications [5]. The major challenges when discussing a HES are its sizing and energy management problems. The sizing problem can be particularly treated as a multi-objective (e.g., cost reduction and battery protection) optimization problem and solved accordingly [6]. In a HES, a number of heterogenous energy sources interact with each other in a distributed manner. Those sources may have very different preferences in operation. They have to work together

© 2018 IEEE. Personal use of this material is permitted. Permission from IEEE must be obtained for all other uses, including reprinting/republishing this material for advertising or promotional purposes, collecting new collected works for resale or redistribution to servers or lists, or reuse of any copyrighted component of this work in other works.

Manuscript received August 21, 2017; revised December 21, 2017, and March 7, 2018; accepted March 28, 2018.

H. Yin is with the Center for Ultra-Wide-Area Resilient Electric Energy Transmission Networks (CURENT), University of Tennessee, Knoxville, TN 37996, USA (e-mail: hyin8@utk.edu).

C. Zhao is with United Automotive Electronic Systems Co., Ltd, Pudong, Shanghai 201206, China (e-mail: chen.zhao3@uaes.com).

C. Ma is with the University of Michigan-Shanghai Jiao Tong University Joint Institute, Shanghai Jiao Tong University, Shanghai 200240, China (e-mail: chbma@sjtu.edu.cn).

in a dynamic environment, in which uncertainties in load demand and system configuration may exist. Due to the failure of a certain source, the configuration of a HES itself may suddenly change to maintain the functionality of the overall system, namely reconfiguration. The classical centralized energy management is known to be inefficient and lack flexibility when handling highly dynamic and distributed systems, such as with unpredictable reconfiguration in topology.

Centralized strategies are popular to manage HESs with a fixed configuration. For example, rule based energy management was applied in a series-parallel plug-in hybrid electric bus, in which the parameters in the rules table were optimized through dynamic programming [7]. Ref. [8] discussed a fuzzy logic based energy management together with rule based control targeting EVs powered by the battery/UC HES. An adaptive fuzzy logic controller was designed to tune the membership functions based on the recorded previous driving conditions. In [9], the energy management problem in a battery/UC HES was solved using Karush-Kuhn-Tucker (KKT) conditions. The two objectives, extension of battery cycle life and maintenance of UC charge/discharge capability, are eventually combined to form a single objective optimization problem. A framework of simultaneous optimal sizing and energy management was proposed to optimally perform onboard energy storage system selection (battery pack, UC pack, or hybrid one), sizing, and power management in a hybrid bus powertrain [10]. Reinforce learning has also been applied in managing a fuel cell/ultracapacitor HES [11].

At the same time, decentralized strategies have also been developed to solve the planning and energy management problems in the HESs and larger systems such as microgrids and smart grids [12], [13]. In terms of decentralized decision making, game theory is a particularly well-known tool that represents the trade-offs among self-interested players and predicts their choices. Interactions among heterogeneous energy sources in a HES were expressed by a non-cooperative game [5]. Distribution of load current was then calculated through iterative solution of Nash equilibrium. Besides the energy management, the capacity allocation of a HES involving wind power and photovoltaic generation is determined and compared by finding the Nash equilibrium in both the non-cooperative game and cooperative game [14]. Comparing with the existing centralized energy managements, the decentralized ones are especially expected to improve the flexibility such as reconfigurability, scalability, reliability and fault-tolerance of HESs. However, so far there is few discussion on control strategies that adapt to the sudden change in the configuration of a HES. This reconfiguration in system topology may happen in real applications when the failure of energy sources happens. There has been a rigorous investigation of fault detection of the key components in HESs, particularly the battery pack [15] [16]. The issue of communication dropouts due to hardware malfunction, cyber attack, etc., has also been addressed [17]. Mostly in HESs involving fuel cells, the fault-tolerance control was developed against motor failure and sensor errors [18], [19]. To the knowledge of the authors, there lacks discussion on a control scheme, particularly in a decentralized manner, that handles the cases when a HES

suddenly reconfigures such as due to the unpredictable failure in its energy sources.

The purpose of this paper is to develop a game theory-based decentralized control strategy for reconfigurable multiple-source HESs. The energy management should be able to be implemented in real time and autonomously adapt to a reconfigured HES. In the case study, a triple-source HES, which contains three heterogeneous energy sources (battery pack, UC pack, and engine-generator) and load, is taken as an example. Similar configurations involving engine generator and energy storage devices have been discussed for shipboard dc power systems, i.e., dc microgrids [10], [20]. As sources of renewable energy, photovoltaic panel and wind turbine are also popular in microgrids. In this paper, the energy sources are first modeled as individual players. The different preferences for the operation of the players are then quantified using their individual utility functions (i.e., satisfaction levels). The energy management problem is represented as a non-cooperative game, in which each player tends to maximize its own utility. However, the satisfaction level of every player also depends on those of others. The solution at each control instant or stage is iteratively reached at the Nash equilibrium via a learning algorithm. This enables the energy management to autonomously adapt to a reconfigured HES in real time. A tuning procedure is also developed to adaptively adjust the weight coefficients in the utility functions. Finally, the performance of the proposed decentralized energy management is validated both through simulation and real-time implementation, during which various possible configurations of the multiple-source HES are switched and tested.

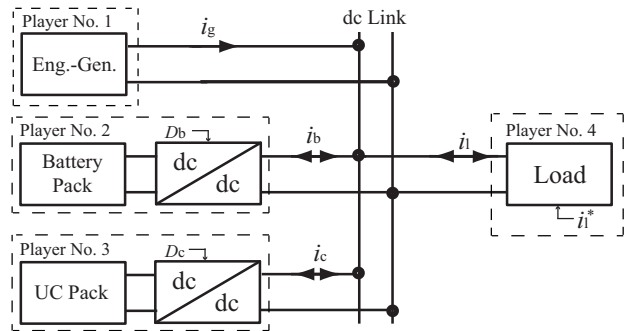


Fig. 1. Configuration of an engine-generator/battery/ultracapacitor HES.

II. CONFIGURATION AND MODELING

In this paper, an engine-generator/battery/ultracapacitor triple-source HES is used as a case study that facilitates the following theoretical discussion. As shown in Fig. 1, the parallel-active topology is employed by which the major devices are connected including the engine-generator, battery pack, UC pack, load, and two bidirectional buck-boost dc-dc converters. It is known that the parallel-active topology provides a higher degree of flexibility and reliability than other topologies [2]. The dc-link voltage can also be maintained within a stable range under the parallel-active topology. Here i_g , i_b , and i_c represent the currents of the engine-generator, battery pack, and UC pack, respectively. The two dc-dc converters work to control the battery current (i_b) and UC

current (i_c), respectively, through the duty cycle control (i.e., D_b and D_c). In battery and energy management, the battery equivalent circuit models are commonly used due to their low computational complexity [5]. In this paper, the battery pack is modeled by its open circuit voltage, internal resistance, and two resistance-capacitance networks. Good agreement between the following simulation and experimental results validates the model accuracy. Meanwhile, it is especially worthy of notice that a high-order physics-based battery model can be simplified to reduce computational effort [21].

Due to the heterogeneity of the sources in the HES, the engine-generator, battery pack, UC pack, and load are modeled as individual players; while the dc link and communication platform (such as a Wi-Fi network in the following experiments) are treated as the environment, in which the players exchange information and power. The players only share their control variables (i.e., i_g , i_b , i_c) and command (i_l^*) with each other through the environment. i_l^* is the load current (i_l) reference command, and physically i_l always equals the sum of i_g , i_b , and i_c . Meanwhile, the local information such as SOCs of the battery pack and UC pack is well preserved internally. Different with the classical centralized control, there is no a main controller. Each player is distributively controlled by its own controller based on the interaction with other players. Note that this decentralized control strategy can be extended to deal with a HES with more sources such as in the application of microgrids. The well-known New European Driving Cycle (NEDC) is chosen as a specific example of dynamic load profiles, as shown in Fig. 2. The NEDC velocity profile is converted into a power profile considering the longitudinal vehicle dynamic of an EV [22]. It should be noted that this load profile can be replaced by any other load profiles such as residential load and industrial load. This paper develops a general scheme for decentralized and scalable control of multiple-source HESs.

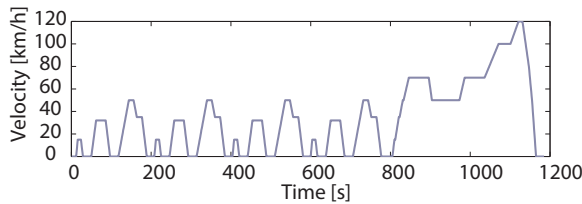


Fig. 2. Example dynamic load profile: New European Driving Cycle (NEDC).

III. FORMULATION OF NON-COOPERATIVE GAME

Here the management of the above multiple-source HES is represented as a multiple-stage non-cooperative game that determines the distribution of the load current. The three energy sources and one energy consumer, namely the engine-generator, battery pack, UC pack, and load, are treated as four individual players with different objectives:

- Engine-generator: maintain a high fuel efficiency;
- Battery pack: extend its own cycle life;
- UC pack: maintain its charging/discharging capability;
- Load: fully meet the load demand.

A. Utility Functions

The objectives of the players are first quantified using their respective utility functions in quadratic form [23]. Note that other types of utility function could also be applied such as logarithmic functions and linear functions [24], [25]. Here quadratic functions are chosen because they are

- a widely used form such as in economics to model the preference of players [13], [23];
- concave functions that guarantee the existence and uniqueness of the Nash equilibrium.

1) *Engine-generator*: It is known that there exists the highest efficiency operating point for an engine-generator, which corresponds to an optimal output current $I_{g,opt}$. Thus the below quadratic utility function u_g is designed to reach its peak value when the actual output current of the engine-generator equals $I_{g,opt}$:

$$u_g = a_g i_g^2 + b_g i_g + c_g. \quad (1)$$

The coefficients, a_g , b_g , and c_g , are listed in Table I. The values of a_g and b_g are taken as -1 and $2I_{g,opt}$, respectively, to maximize u_g when i_g equals $I_{g,opt}$ (i.e., the preference of the engine-generator), and c_g is designed to normalize the maximum of u_g as one. All the coefficients in the below utility functions, (2)(4) and (6), are similarly determined.

TABLE I
COEFFICIENTS OF UTILITY FUNCTIONS.

	a_x	b_x	c_x
Engine generator (g)	-1	$2I_{g,opt}$	$1-I_{g,opt}^2$
Battery pack (b)	-1	$I_{b,ave} + I_{b,l}$	$1-I_{b,ave}^2 - I_{b,l}^2$
UC pack (c)	-1	$2I_{c,fit}$	$1-I_{c,fit}^2$
Load (l)	-1	$2(i_g + i_b + i_c)$	$1-(i_g + i_b + i_c)^2$

2) *Battery Pack*: The utility function of the battery pack u_b is defined to emphasize the extension of the battery cycle life, namely suppression of the variation in its output current. Again, a quadratic function is applied,

$$u_b = a_b i_b^2 + b_b i_b + c_b, \quad (2)$$

where a_b , b_b , and c_b have a similar definition as the ones for the engine-generator. b_b here is a parameter which relates to $I_{b,ave}$ and $I_{b,l}$, the average battery current so far and the battery current at the last control instant, respectively. The utility function u_b is maximized when the present battery current i_b equals $(I_{b,ave} + I_{b,l})/2$, namely a smooth output current from the battery pack. Note that the battery cycle life is largely determined by the values of the battery current and temperature [26]. The relationship between the battery current and cycle life can be represented as follows,

$$Q_{b,loss} = Ae^{-\frac{E_a + BC_{Rate}}{RT_b}} (A_h)^Z, \quad (3)$$

where $Q_{b,loss}$ is the loss of battery capacity due to the ageing [27]. A , B , and Z are parameters achieved through fitting the experimental data; C_{Rate} is discharging rate; E_a is activation energy; R is gas constant; T_b is battery temperature; and A_h is Ah-throughput. In the following simulation and experiments, all these parameters of the battery pack are experimentally calibrated [see Table II]. Note that here the initial capacity of the battery is normalized to one.

TABLE II
PARAMETERS OF BATTERY AGEING MODEL.

A	B	Z	E_a	R	T_b
-	-	-	J	J/(mol·K)	K
600	-140	0.55	30195	8.314	298

3) *Ultracapacitor Pack*: The utility function of the UC pack u_c is expressed as follows,

$$u_c = a_c i_c^2 + b_c i_c + c_c, \quad (4)$$

where a_c , b_c , and c_c are also listed in Table I. The purpose of having a UC pack is to serve as an energy buffer. Thus the preference of the UC pack is to maintain its SOC level at a certain preferred value. Thus it is always capable to quickly deliver or absorb power. The parameter b_c can then be defined to be proportional to $I_{c,fit}$,

$$I_{c,fit} = \left(2 \frac{v_c - V_{c,min}}{V_{c,max} - V_{c,min}} - 1 \right) I_{c,max}, \quad (5)$$

where v_c , $V_{c,min}$, $V_{c,max}$, and $I_{c,max}$ are the voltage, minimum voltage, maximum voltage, and maximum current of the UC pack. The current $I_{c,fit}$ directly relates to the SOC of the UC pack. Assuming an equal possibility of charge and discharge, $I_{c,fit}$ is designed targeting a 50% UC SOC. The above UC SOC control also helps to improve the energy efficiency because the large UC internal resistance and low output voltage can be avoided when the UC SOC is low [28].

4) *Load*: As an energy consumer, ideally the load command i_l^* should equal the sum of the actual output currents from the three energy sources when they are all in operation. Thus the utility function for the load u_l is defined as

$$u_l = a_l i_l^{*2} + b_l i_l^* + c_l, \quad (6)$$

where a_l , b_l , and c_l are coefficients and given in Table I. The above utility function is maximized when i_l^* exactly equals $(i_g + i_b + i_c)$, which again is represented by b_l .

5) *Final Form of Utility functions*: Note that the utility function for the load only contains the control variables of the energy sources, i.e., i_g , i_b , and i_c . Thus the load should not be treated as a fully independent player because it has no its own control variable. It only shares the reference command i_l^* . A possible solution is to combine the utility of the load with those of energy sources. Thus the final form of the utility functions is modified as follows,

$$u_{g,l} = w_g u_g + w_{l,g} u_l, \quad (7)$$

$$u_{b,l} = w_b u_b + w_{l,b} u_l, \quad (8)$$

$$u_{c,l} = w_c u_c + w_{l,c} u_l, \quad (9)$$

where w_g , w_b , w_c , $w_{l,g}$, $w_{l,b}$, and $w_{l,c}$ are weight coefficients. As explained in section III-C, the first three coefficients are determined later via an adaptive tuning procedure because both a specific load profile and reconfiguration (such as due to the failure of a certain energy source) influence their optimal values, while the last three ones are treated as penalty factors. The physical meaning of the above final form of the utility functions is that each energy source works to satisfy its own preference, but at the same time it is required to contribute to

meeting the desired condition of $i_l^* = i_g + i_b + i_c$ as much as possible. Note that in real applications, a specific energy source may fail and then quit the non-cooperative game, thus the below relationship,

$$i_l^* \geq i_g + i_b + i_c, \quad (10)$$

holds. Note that here i_l^* is the reference load command, not the actual load current. When failures happen, the sum of i_g , i_b , and i_c may be lower than i_l^* , i.e., the derated operation mode discussed in sections IV and V.

B. Nash Equilibrium

A non-cooperative game is then set up at each stage (i.e., control instant). The game determines the load current distribution among the three energy sources. It is represented in the strategic form,

$$G_{pd} = \{(G, B, C), \{i_g, i_b, i_c\}, \{u_{g,l}, u_{b,l}, u_{c,l}\}\}. \quad (11)$$

In the above form, each independent player, i.e., the engine-generator (“G”), battery pack (“B”), or UC pack (“C”), is assumed to be selfish, and thus it attempts to maximize its own utility. However, the final value of utility function of a single player, $u_{g,l}$, $u_{b,l}$, or $u_{c,l}$, is determined not only by its own control variable but also by control variables of others and reference load command due to the interactions occurring in the environment, i.e., the relationship described in (6) and (10). Since the three independent players are selfish, a balanced distribution of the load current settles down at the so-called “Nash equilibrium” at each stage. Note that here a single stage (i.e., at each control instant) is treated as an independent game because the future load demand is assumed to be unpredictable. Under the Nash equilibrium, all the players’ utilities can not be improved if one of the players unilaterally changes its decision/control variable (i.e., i_g , i_b , or i_c). Due to the concavity of the utility functions, $u_{g,l}$, $u_{b,l}$, and $u_{c,l}$, the existence and uniqueness of a Nash equilibrium can be straightforwardly proved by solving the following best response (BR) functions,

$$BR_g : \frac{\partial u_{g,l}}{\partial i_g} = 0, BR_b : \frac{\partial u_{b,l}}{\partial i_b} = 0, BR_c : \frac{\partial u_{c,l}}{\partial i_c} = 0. \quad (12)$$

The detailed proof of the existence and uniqueness of the Nash Equilibrium is omitted here. Note that in the below discussions, one or two energy sources are allowed to quit the game such as due to failure, namely reconfiguration of the HES. Thanks to the concavity of all the three utility functions, the new Nash equilibrium still exists and is unique when there are two functional energy sources, i.e., with one failed energy source.

The purpose of this paper is to develop a decentralized energy management strategy that autonomously adapts to the reconfigured HES. Through the environment, each player shares its decision, i.e., control variable (i_g , i_b , or i_c), while its internal information such as the SOC is internally preserved. As shown in Algorithm 1, a learning algorithm is developed for each stage using the engine-generator as an example. The other two players apply the same algorithm. In the

initialization step, each player shares its decision made at the last stage, namely $i_{g,k-1}$, $i_{b,k-1}$, and $i_{c,k-1}$. k represents present number of stage. For the engine-generator, in order to maximize its own utility function $u_{g,l}$, its decision i_g is solved using its own best response function,

$$BR_g : w_g(2a_g i_g + b_g) + w_{l,g} [2i_l^* - 2(i_g + i_b + i_l)] = 0, \quad (13)$$

which is initially under given $i_b = i_{b,k-1}$ and $i_c = i_{c,k-1}$. Note that i_l^* is the newest load command. The same procedure repeats in the players of battery pack and UC pack, which in turn updates their respective decisions (i_b and i_c). i_g is then iteratively calculated using (13) and with updated i_b and i_c until it converges to a stable value. At the same time, the convergence of i_b and i_c also iteratively achieves, namely the Nash equilibrium of the non-cooperative game [see Fig. 3]. Due to the linearity of the response functions such as (13), the solution of the Nash equilibrium is expected to be fast enough to be implemented in real time, as validated in section V. All the three players continue to operate at the Nash equilibrium until the load demand changes and then they move to the next stage of the game, i.e., convergence to a new Nash equilibrium.

Algorithm 1 Algorithm to reach Nash Equilibrium

1. Initialization

$$i_{g,last} \leftarrow i_{g,k-1}, i_b \leftarrow i_{b,k-1}, i_c \leftarrow i_{c,k-1}$$

2. Learning Phase

Solve $BR_g(i_g, i_b, i_c)$ for i_g

3. Check Phase

if $|i_g - i_{g,last}| < \varepsilon$ then

Go to step 4. Termination

else

1) $i_{g,last} \leftarrow i_g$

2) Wait for updated i_b and i_c from other two players

3) Go to step 2. Learning Phase

end if

4. Termination

$$i_{g,k} \leftarrow i_g$$

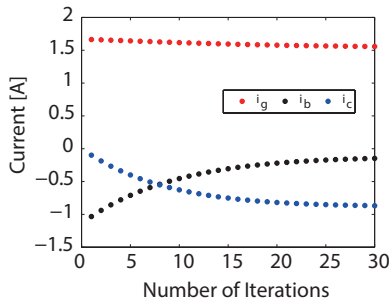


Fig. 3. Convergence of decisions of the three players at an example stage in the following simulation, Section IV.

C. Adaptive Tuning of Weight Coefficients

It is desirable that the weight coefficient for each player can be also determined by the player itself. The values of the weight coefficients are expected to be adaptively adjusted under different cycles as well as with different combinations of

the energy sources such as when possible failure happens. An initial optimal set of weight coefficients can be first determined targeting a specific cycle, such as the example NEDC cycle. This initial set can be solved through a multi-objective genetic algorithm, as discussed in the following paragraph [29]. Here the multiple objectives during an entire single cycle are $Q_{b,loss}$ defined in (3), and

$$C_{g,ave} = \frac{\sum C_g}{N}, \quad (14)$$

$$SOC_{c,ave} = \frac{\sum SOC_c}{N}, \quad (15)$$

$$I_{dif,ave} = \frac{\sum |i_l^* - (i_g + i_b + i_c)|}{N}, \quad (16)$$

where N is the total number of the control instants; $C_{g,ave}$ is the average fuel consumption of the engine-generator; $SOC_{c,ave}$ is the average SOC of the UC pack; and $I_{dif,ave}$ is the average difference between the load demand and actual total load current provided by the energy sources. The weight coefficients, w_g , w_b , and w_c , are adaptively tuned by the individual players according to their own utilities [refer to (7)-(9)]. A basic idea is that when the utility of a specific player is low, the player will increase its weights and vice versa. Note that similar tuning method has been widely applied in tuning inertia weight of particle swarm optimization (PSO) [30].

In the present case study, $w_{l,g}$, $w_{l,b}$, and $w_{l,c}$ are treated as penalty factors because it is a high priority request that the sum of i_g , i_b , and i_c should be as close as possible to i_l^* . Thus a large value such as 10 is chosen for $w_{l,g}$, $w_{l,b}$, and $w_{l,c}$. This way of determining penalty factors is a common practice for optimization algorithms [31]. With the given values of the penalty factors, the tradeoff relationship among the initial w_g , w_b , and w_c can be represented by the so-called Pareto set. It is known that the knee point of the Pareto-optimal front, which is determined through the multi-objective genetic algorithm, gives the most satisfactory solution among the above three objectives/criteria, $C_{g,ave}$, $Q_{b,loss}$, and $SOC_{c,ave}$ [9]. Note that the objective of suppressing $I_{dif,ave}$ is reflected by the penalty factors. The initial values of all the six weight coefficients are listed in Table III. The three weight coefficients, w_g , w_b , and w_c , are then adaptively tuned as follows taking w_g as an example,

- If $|i_g - I_{g,opt}| \geq \Theta_g$,
then $w_g \leftarrow \max[\min(w_{g,max}, w_g + \Delta w_g), w_{g,min}]$,
- If $|i_g - I_{g,opt}| < \Theta_g$,
then $w_g \leftarrow \max[\min(w_{g,max}, w_g - \Delta w_g), w_{g,min}]$,

where Θ_g stands for the threshold value; $w_{g,max}$ and $w_{g,min}$ are the upper bound and lower bound, respectively; Δw_g is the tuning step size. The difference between the preference parameter $I_{g,opt}$ and control variable i_g is used to indicate the satisfaction level of the utility of the engine-generator. All the parameters for the tuning of the weight coefficients are summarized in Table III. As shown in (6) and Table I, the sum of the output currents of the energy sources is expected to be as equal as the load current command. This requirement is represented by the large $w_{g,l}$, $w_{b,l}$, and $w_{c,l}$ comparing with w_g , w_b , and w_c . If one or two sources fail, i.e., with zero output current, the new Nash equilibrium will be reached through the

learning algorithm developed in the above subsection. Note that since the UC pack is an energy buffer due to its limited energy density, it is not allowed to work as a sole energy source.

TABLE III
DETERMINATION OF WEIGHT COEFFICIENTS.

Initial Values		Adaptive Tuning		
w_g	$w_{l,g}$	$w_{g,max}$	$w_{g,min}$	Δw_g
0.9	10	1	0.8	0.001
w_b	$w_{l,b}$	$w_{b,max}$	$w_{b,min}$	Δw_b
0.4	10	0.5	0.3	0.001
w_c	$w_{l,c}$	$w_{c,max}$	$w_{c,min}$	Δw_c
0.1	10	0.2	0	0.001

IV. SIMULATION RESULTS

Simulation is conducted targeting the following downscaled experimental system in section V. For a quantitative evaluation, the above four criteria, $C_{g,ave}$, $Q_{b,loss}$, $SOC_{c,ave}$, and $I_{dif,ave}$, are applied. Each of them directly corresponds to its respective utility function [refer to (1), (2), (4), and (6)]. In the simulation and following experiments, the size of the battery pack is determined to supply the one-third of the average power in the example NEDC cycle, and the engine-generator, a major energy source, provides the rest two-thirds when operating at its maximum efficiency point, i.e., with the output current of $I_{g,opt}$. As an energy buffer, the UC pack is configured to supply all the dynamic load current between 904–1130 s in the NEDC cycle using the half of the UC pack’s total capacitance [see Fig. 2]. Note that in the example NEDC cycle, the period between 904–1130 s requires the fastest and longest acceleration, i.e., a large dynamic load current.

A. Static Cases

Six different static cases (i.e., different combinations of the energy sources) are investigated, namely with a fixed configuration. For space conservation, only the current responses for the combinations of GBC and BC are shown in Fig. 4(a) and (b), respectively. Again “G”, “B”, and “C” denote the engine-generator, battery pack, and UC pack, respectively. These two example combinations, “GBC” and “BC”, represent, respectively, normal operation and pure-electric derated operation when the engine-generator fails. In the derated operation mode, the maximum output current of the battery is limited, 5 A in the simulation. Note that as an energy buffer, the UC pack is not allowed to operate alone.

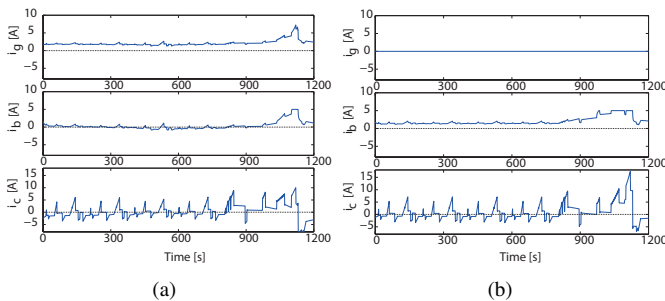


Fig. 4. Example current responses of i_g , i_b , and i_c . (a) “GBC”. (b) “BC”.

The results of the four criteria are summarized in Table IV, which are calculated for a single NEDC cycle. All the six possible combinations of the energy sources are under the game theory-based decentralized control. The performance of the “GBC” combination is obviously the best. As shown in Fig. 4(a), the engine-generator provides a stable output current; the battery pack covers the slow dynamic current; and the UC pack contributes the rest high dynamic current. When one of the energy sources does not involve such as the engine-generator in Fig. 4(b), the remaining two energy sources (i.e., battery pack and UC pack) have to change their strategies. A relative low performance is shown in Table IV when comparing the other five combinations with the “GBC” combination. It is natural that the two cases with a single energy source (“G” and “B”) have the poorest performance. Note that in these two derated cases, either the engine-generator or battery pack is assumed to incapable to meet the entire load demand alone. As shown in Fig. 5, the SOC of the UC pack SOC_c is well controlled to be close to 50% in the “GBC”, “BC”, and “GC” combinations unless it has to apply a large dynamic current at the end of the NEDC cycle, i.e., the period between 904–1130 s. Meanwhile, the UC SOC starts to recover after this period, namely from 1130 s.

TABLE IV
VALUES OF CRITERIA IN A SINGLE NEDC CYCLE.

	$C_{g,ave}$ (L/kWh)	$Q_{b,loss}$ (J)	$SOC_{c,ave}$ (%)	$I_{dif,ave}$ (A)
GBC	0.2621	1.47e-6	54.90	0.0219
BC	-	1.77e-6	52.90	0.0251
GB	0.3171	1.72e-6	-	0.1025
GC	0.2948	-	47.66	0.0345
G	0.5000	-	-	0.6438
B	-	1.96e-6	-	0.4026

TABLE V
ADAPTIVE TUNING VERSUS STATIC WEIGHTS (“GBC” CASE).

	$C_{g,ave}$ (L/kWh)	$Q_{b,loss}$ (J)	$SOC_{c,ave}$ (%)	$I_{dif,ave}$ (A)
Static	0.2650	1.50e-6	57.23	0.0225
Adaptive	0.2621 (1.09%↓)	1.47e-6 (2.00%↓)	54.90 (4.07%↓)	0.0219 (2.67%↓)

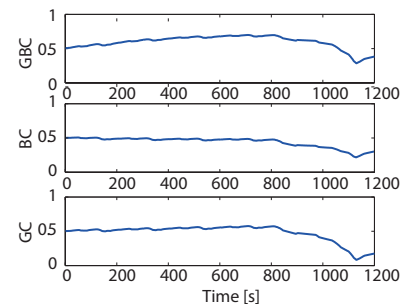


Fig. 5. UC SOC responses.

For reference purposes, the criteria are compared when using adaptive weight tuning and the static weights (i.e., the initial values in Table III), taking the “GBC” combination as an example. As shown in Table V, the results using the adaptive tuning clearly show an improved performance. Additionally,

Fig. 6 shows the normalized battery pack capacity evolution profiles [refer to Section III-A2]. In the figure, one cycle includes ten continuous discharge profiles in Fig. 4(a) (i.e., i_b) and later three-hour full charge. The scenario of “baseline” refers to the case in which the battery pack provides the entire load current, i.e., a conventional battery alone system. As expected, the present triple-source HES obviously reduces the battery degradation under the proposed control. Table VI summarizes the average energy efficiencies, again taking the “GBC” case as an example. η_b and η_c are the efficiencies of the battery pack and UC pack, respectively. The energy management here is a multi-objective one including the improvement in energy efficiencies, i.e., energy saving, as discussed in Section III-A1 and III-A3.

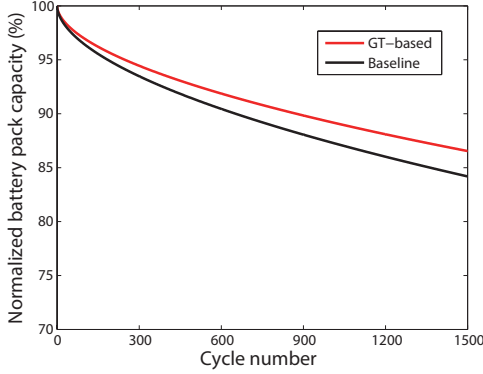


Fig. 6. Battery pack capacity evolution with cycling (“GBC” case).

TABLE VI
AVERAGE ENERGY EFFICIENCIES (“GBC” CASE).

$C_{g,ave}$ (L/kWh)	η_b (%)	η_c (%)
0.2621	97.85%	92.59%

B. Dynamic Cases

In real applications, some of the energy sources may suddenly fail and thus be cut off during the operation. The dynamic case simulates a realistic situation when the engine-generator and UC pack are cut off one by one. It is challenging because in the example triple-source energy system, the engine-generator is a major source of energy. As shown in Fig. 7, the engine-generator is cut off at 400 s (i.e., $i_g = 0$), and then the UC pack quits at 800 s (again, $i_c = 0$). The configuration changes from the original engine-generator/battery/UC HES to a battery/UC HES and eventually a battery-alone system. Thanks to the decentralized nature of the game theory-based control, the energy system autonomously adapts to the sudden change in its configuration. The battery pack automatically supplies a large current after 400 s with the sudden absence of the engine-generator; and it solely works in the derated operation mode when the UC pack also fails at 800 s. Besides the dynamic current, the UC pack also contributes to the average load current between 400–800 s, namely the continuous discharge shown in its SOC response in Fig. 7. Note that in order to maintain an optimal output

TABLE VII
GT-BASED CONTROL VERSUS CENTRALIZED CONTROL.

Control	$C_{g,ave}$ (L/kWh)	$Q_{b,loss}$ (J)	$SOC_{c,ave}$ (%)	$I_{dif,ave}$ (A)	t_{sim} (s)
-	0.2621	1.47e-6	54.90	0.0219	0.84
GT-based	0.2600	1.38e-6	60.63	0	31.39
Centralized					

current (i.e., high fuel economy) of the engine-generator, the UC pack is slightly charged before 400 s. Here it is assumed that the controllers of the players, namely the energy sources, are still functional despite the failures of the players themselves. The other possible dynamic cases are similar and thus the descriptions are omitted to avoid redundancy.

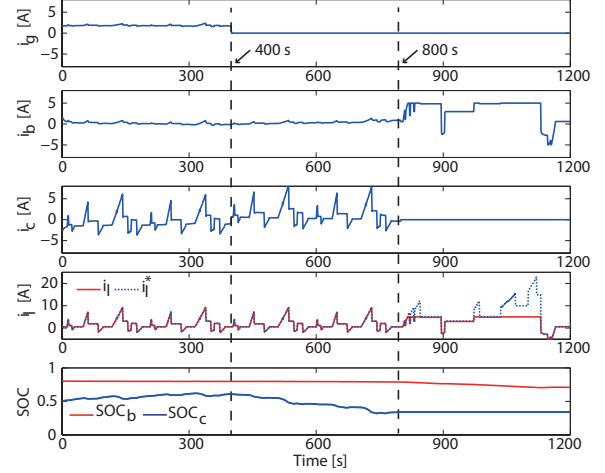


Fig. 7. Current and SOC responses in example dynamic case (from “GBC” to “BC” and then “B”).

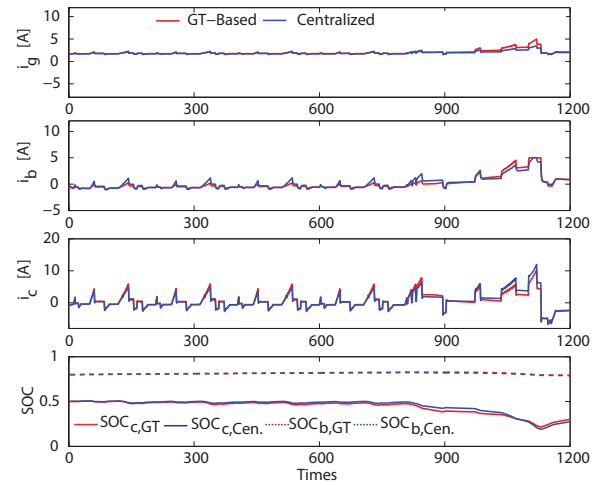


Fig. 8. Current and SOC responses under GT-based control and centralized control.

C. Comparison with Centralized Control

The game theory-based decentralized control is compared with centralized control, in which the control problem is also based on the utility functions but formed through the weight-sum method [32]. Note that the weight-sum method is a typical approach to transform a multi-objective optimization problem into a single-objective optimization problem. The initial values of the six weights in Table III are applied. The optimization problem is then solved through sequential

quadratic programming (SQP), a popular iterative method for nonlinear optimization [33].

The simulation results under the ‘‘GBC’’ combination are shown and summarized in Fig. 8 and Table VII, respectively. The game theory (GT)-based decentralized control demonstrates comparable performance to that of the centralized controls in terms of both current/SOC responses and the first four criteria in Table VII. Thanks to the decentralized nature, the required computational power of the game theory-based control is much lower. It leads to much shorter overall execution time when calculating over the same simulation (Matlab/Simulink) and hardware platform [see t_{sim} in the last column of Table VII]. Unlike the centralized control, the proposed game theory-based decentralized control is capable to autonomously adapt to the variation in the system configuration, as explained in the above two subsections.

D. Scalability

The enhanced scalability of the energy management is particularly expected to be an important advantage for applying the game theory-based decentralized control. In this paper, the triple source engine-generator/battery/ultracapacitor HES is used as a case study. However, the proposed control scheme itself is general for energy systems with more sources. Thus for verification purposes, in the simulation the number of the battery pack (with identical parameters) is assumed to increase from 3 to 100. Figure 9 shows the numbers of iterations required to reach the convergence of all the control variables (i.e., the output currents from the sources) at an example stage or control instant [refer to sec. III-B]. Under the game theory-based decentralized control, the convergence speed does not substantially increase such as with exponential increment. This result further verifies the advantages of the proposed decentralized control in terms of scalability and computational efficiency. Note that there is a tradeoff between the value of threshold ε and convergence speed. The threshold could be treated as a design parameter for a specific target application.

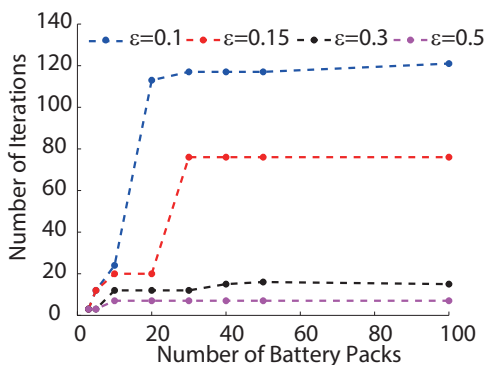


Fig. 9. Number of iterations under different number of battery pack and various values of threshold.

V. EXPERIMENTAL IMPLEMENTATION

A down scaled test bench was built up to match the power capability of the devices in the experimental system. The test bench has the same configuration with the one in Fig. 1. As shown in Fig. 10, the load profile, i.e., NEDC here, is emulated

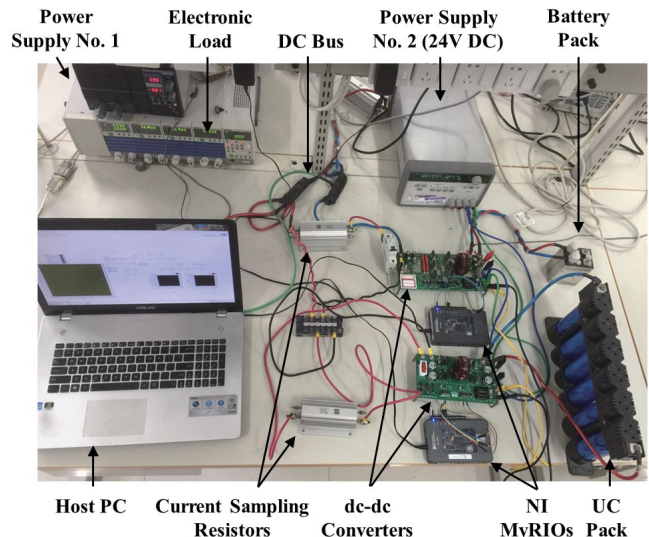


Fig. 10. A down scaled test bench for the triple-source HES.

TABLE VIII
SPECIFICATIONS OF TEST BENCH.

Li-ion battery pack (Lishen LP2770102AC)	Two cells (series), 12.5 Ah/cell, 3.2 V/cell (Nominal Vol.)
UC pack (Nippon Chemi-Con DLE series)	Six cells (series) 1760 F/cell, 2.5 V/cell (Max Vol.)
Two dc-dc converters (Design/fabricate in house)	Peak power: 100 W and 400 W Switch frequency: 20 kHz
Electronic load (Kikusui PLZ-50F/150U)	Max power: 600 W (1 PLZ-50F, 4 PLZ150Us with 1.5–150 V 0–30 A each)
Power supply No. 1 (Takasago ZX-800L)	Max power: 800 W 0–80 V, 0–80 A
Current sampling resistors (PCN Corporation RH series)	Three RH250M4: 0.01 Ω Accuracy: $\pm 0.02\%$

through the combination of the power supply No. 1 and electronic load; the engine-generator model is implemented in the host PC, namely a virtual player of engine-generator in the setup. This virtual implementation of the engine-generator, i.e., hardware-in-loop (HIL) simulation, is a common practice in existing research [34]. The specifications of the battery pack, UC pack, dc-dc converters, electronic load, and power supplies are listed in Table VIII. The two dc-dc converters work in current-control mode.

The two National Instruments (NI) myRIO controllers collect data and calculate the output currents of the two real players (the battery pack and UC pack), namely the current reference commands of the two bi-directional buck-boost dc-dc converters connected with the packs, respectively. As explained above, the controller of the engine-generator is virtually implemented in the host PC. Note that here one single myRIO only deals with its own player, i.e., a decentralized control configuration. The load current distribution is updated at each control instant with an interval of 1 s. The three controllers of the players (two myRIOS and one host PC) determine the output currents from their respective players, i.e., the Nash equilibrium reached through the proposed learning algorithm. The controllers communicate with each other through a Wi-Fi network.

As shown in Fig. 11, the current and voltage responses

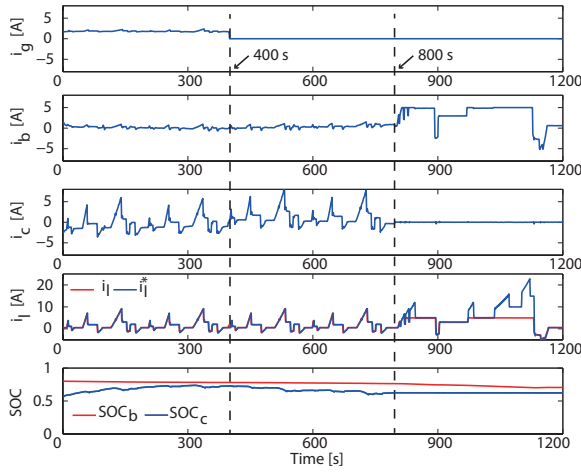


Fig. 11. Experimental current and SOC responses in example dynamic case (from “GBC” to “BC” and then “B”).

TABLE IX
CRITERIA IN SIMULATION AND EXPERIMENTS.

	$C_{g,ave}$ (L/kWh)	$Q_{b,loss}$ (J)	$SOC_{c,ave}$ (%)	$I_{dif,ave}$ (A)
Experiments	0.2694	1.52e-06	45.69	1.0777
Simulation	0.2684	1.51e-06	45.71	0.8484

in experiments well match those in the simulation when the engine-generator and UC pack are cut off at 400 s and 800 s, respectively [see Fig. 7]. This validates the above theoretical discussion and real-time implementation of the proposed game theory-based control. Again, in experiments the engine-generator provides an almost constant output current that corresponds to its optimal fuel economy; the battery pack becomes a major source when the engine-generator is cut off from 400 s; the UC pack supplies the most of the dynamic load demand before it quits at 800 s. The required load is fully met until the system enters the derated operation mode, i.e., the battery-alone case. The values of the four criteria, average fuel consumption, battery capacity loss, average UC SOC, and average battery current difference in the single NEDC cycle are co-listed with the simulation results. As shown in Table IX, the two results well match each other. The small differences between the simulation and experimental results are mainly due to the unavoidable sample errors and extra energy losses in circuits and wires in real experiments.

VI. CONCLUSION

This paper develops a decentralized energy management strategy for reconfigurable multiple-source energy systems. It uses the engine-generator/battery/UC HES as a case study. The energy management problem is treated as a non-cooperative game, in which the engine-generator, battery pack, UC pack, and load are modeled as individual players. Each player possesses a utility function quantifying its unique preference in actual operation, i.e., improving fuel economy, extending battery cycle life, maintaining UC charging/discharge capability, or meeting load demand. Through a learning algorithm,

the Nash equilibrium is iteratively reached and updated to determine a balanced load current distribution among the players. A tuning procedure is also included to make the weight coefficients in the utility functions adaptive to the present cycle and configuration of the example HES. Both the simulation and experimental results validate the improved flexibility and scalability when applying the game theory-based energy management. This decentralized control also demonstrates comparable performance to that of the classical centralized control.

The proposed approach (i.e., combination of multi-agent modeling and game theory-based control) could be further extended to solve the energy management problem in other HESs involving more heterogeneous “players” such as a microgrid, which is prone to communication dropouts, failures, etc. Again, for such systems, control strategies are required to effectively deal with the dynamic power (e.g., wind and solar) and load (e.g., buildings and EVs) profiles, different natures/preferences of the components involved, possible re-configuration of the overall system such as due to failures or applications themselves (e.g., changing number of plugged in EVs), etc. This paper provides a foundation to further address the above issues when managing more complicated HESs including the microgrids.

REFERENCES

- [1] S. Ashok, “Optimised model for community-based hybrid energy system,” *Renew. energy*, vol. 32, no. 7, pp. 1155–1164, 2007.
- [2] A. Kuperman and I. Aharon, “Battery–ultracapacitor hybrids for pulsed current loads: A review,” *Renew. Sustain. Energy Rev.*, vol. 15, no. 2, pp. 981–992, 2011.
- [3] L. Zhang, X. Hu, Z. Wang, F. Sun, and D. G. Dorrell, “A review of supercapacitor modeling, estimation, and applications: A control/management perspective,” *Renew. Sust. Energy Rev.*, 2017.
- [4] —, “Fractional-order modeling and state-of-charge estimation for ultracapacitors,” *J. Power Sources*, vol. 314, pp. 28–34, 2016.
- [5] H. Yin, C. Zhao, M. Li, C. Ma, and M.-Y. Chow, “A game theory approach to energy management of an engine-generator/battery/ultracapacitor hybrid energy system,” *IEEE Trans. Ind. Electron.*, vol. 63, no. 7, pp. 4266–4277, Jul. 2016.
- [6] L. Zhang, X. Hu, Z. Wang, F. Sun, J. Deng, and D. Dorrell, “Multi-objective optimal sizing of hybrid energy storage system for electric vehicles,” *IEEE Trans. Veh. Technol.*, vol. 67, no. 2, pp. 1027–1035, Feb 2018.
- [7] J. Peng, H. He, and R. Xiong, “Rule based energy management strategy for a series–parallel plug-in hybrid electric bus optimized by dynamic programming,” *Applied Energy*, 2016.
- [8] H. Yin, W. Zhou, M. Li, C. Ma, and C. Zhao, “An adaptive fuzzy logic-based energy management strategy on battery/ultracapacitor hybrid electric vehicles,” *IEEE Trans. Transport. Electrification*, vol. 2, no. 3, pp. 300–311, Sep. 2016.
- [9] H. Yin, C. Zhao, M. Li, and C. Ma, “Utility function-based real-time control of a battery ultracapacitor hybrid energy system,” *IEEE Trans. Ind. Informat.*, vol. 11, no. 1, pp. 220–231, Feb. 2015.
- [10] X. Hu, N. Murgovski, L. M. Johannesson, and B. Egardt, “Comparison of three electrochemical energy buffers applied to a hybrid bus powertrain with simultaneous optimal sizing and energy management,” *IEEE Trans. Intell. Transp. Syst.*, vol. 15, no. 3, pp. 1193–1205, 2014.
- [11] W.-S. Lin and C.-H. Zheng, “Energy management of a fuel cell/ultracapacitor hybrid power system using an adaptive optimal-control method,” *J. Power Sources*, vol. 196, no. 6, pp. 3280–3289, 2011.
- [12] J. von Appen, T. Stetz, M. Braun, and A. Schmiegel, “Local voltage control strategies for PV storage systems in distribution grids,” *IEEE Trans. Smart Grid*, vol. 5, no. 2, pp. 1002–1009, Mar. 2014.
- [13] W. Shi, X. Xie, C.-C. Chu, and R. Gadh, “Distributed optimal energy management in microgrids,” *IEEE Trans. Smart Grid*, vol. 6, no. 3, pp. 1137–1146, May 2015.

- [14] S. Mei, Y. Wang, F. Liu, X. Zhang, and Z. Sun, "Game approaches for hybrid power system planning," *IEEE Trans. Sustain. Energy*, vol. 3, no. 3, pp. 506–517, Jul. 2012.
- [15] B. Xia, Y. Shang, T. Nguyen, and C. Mi, "A correlation based fault detection method for short circuits in battery packs," *J. Power Sources*, vol. 337, pp. 1–10, 2017.
- [16] Z. Liu and H. He, "Sensor fault detection and isolation for a lithium-ion battery pack in electric vehicles using adaptive extended kalman filter," *Applied Energy*, vol. 185, no. 2, pp. 2033–2044, 2017.
- [17] Y. Liu, H. Xin, Z. Qu, and D. Gan, "An attack-resilient cooperative control strategy of multiple distributed generators in distribution networks," *IEEE Trans. Smart Grid*, vol. 7, no. 6, pp. 2923–2932, 2016.
- [18] H. Aouzellag, K. Ghedamsi, and D. Aouzellag, "Energy management and fault tolerant control strategies for fuel cell/ultra-capacitor hybrid electric vehicles to enhance autonomy, efficiency and life time of the fuel cell system," *Int. J. Hydrogen Energy*, vol. 40, no. 22, pp. 7204–7213, 2015.
- [19] L. Xu, J. Li, M. Ouyang, J. Hua, and X. Li, "Active fault tolerance control system of fuel cell hybrid city bus," *Int. J. Hydrogen Energy*, vol. 35, no. 22, pp. 12510–12520, 2010.
- [20] Z. Jin, G. Sulligoi, R. Cuzner, L. Meng, J. C. Vasquez, and J. M. Guerrero, "Next-generation shipboard dc power system: Introduction smart grid and dc microgrid technologies into maritime electrical networks," *IEEE Electrification Magazine*, vol. 4, no. 2, pp. 45–57, 2016.
- [21] C. Zou, C. Manzie, and D. Nešić, "A framework for simplification of PDE-based lithium-ion battery models," *IEEE Trans. Control Syst. Technol.*, vol. 24, no. 5, pp. 1594–1609, 2016.
- [22] C. Ma, M. Xu, and H. Wang, "Dynamic emulation of road/tyre longitudinal interaction for developing electric vehicle control systems," *Veh. Syst. Dynam.*, vol. 49, no. 3, pp. 433–447, 2011.
- [23] N. Rahbari-Asr, M.-Y. Chow, J. Chen, and R. Deng, "Distributed real-time pricing control for large scale unidirectional V2G with multiple energy suppliers," *IEEE Trans. Ind. Informat.*, vol. 12, no. 5, pp. 1953–1962, Oct. 2016.
- [24] W. Tushar, B. Chai, C. Yuen, D. B. Smith, K. L. Wood, Z. Yang, and H. V. Poor, "Three-party energy management with distributed energy resources in smart grid," *IEEE Trans. Ind. Electron.*, vol. 62, no. 4, pp. 2487–2498, 2015.
- [25] L. Ma, N. Liu, J. Zhang, W. Tushar, and C. Yuen, "Energy management for joint operation of CHP and PV prosumers inside a grid-connected microgrid: A game theoretic approach," *IEEE Trans. Ind. Informat.*, vol. 12, no. 5, pp. 1930–1942, Oct. 2016.
- [26] C. Zhao, H. Yin, and C. Ma, "Quantitative evaluation of LiFePO battery cycle life improvement using ultracapacitors," *IEEE Trans. Power Electron.*, vol. 31, no. 6, pp. 3989–3993, Jun. 2016.
- [27] Z. Song, J. Li, X. Han, L. Xu, L. Lu, M. Ouyang, and H. Hofmann, "Multi-objective optimization of a semi-active battery/supercapacitor energy storage system for electric vehicles," *Applied Energy*, vol. 135, pp. 212–224, 2014.
- [28] O. Laldin, M. Moshirvaziri, and O. Trescases, "Predictive algorithm for optimizing power flow in hybrid ultracapacitor/battery storage systems for light electric vehicles," *IEEE Trans. Power Electron.*, vol. 28, no. 8, pp. 3882–3895, Aug. 2013.
- [29] L. Zhang, L. Wang, G. Hinds, C. Lyu, J. Zheng, and J. Li, "Multi-objective optimization of lithium-ion battery model using genetic algorithm approach," *J. Power Sources*, vol. 270, pp. 367–378, 2014.
- [30] G. Xu, "An adaptive parameter tuning of particle swarm optimization algorithm," *Appl. Math. Comput.*, vol. 219, no. 9, pp. 4560–4569, 2013.
- [31] S. S. Rao and S. S. Rao, *Engineering optimization: theory and practice*. John Wiley & Sons, 2009.
- [32] J. Arora, *Introduction to optimum design*. Academic Press, 2004.
- [33] P. T. Boggs and J. W. Tolle, "Sequential quadratic programming," *Acta Numer.*, vol. 4, pp. 1–51, 1995.
- [34] S. G. Li, S. Sharkh, F. C. Walsh, and C.-N. Zhang, "Energy and battery management of a plug-in series hybrid electric vehicle using fuzzy logic," *IEEE Trans. Veh. Technol.*, vol. 60, no. 8, pp. 3571–3585, Oct. 2011.



phasor measurement unit (PMU) design.

He Yin (S'13-M'16) received the B.S. and Ph.D. degrees in electrical and computer engineering from University of Michigan-Shanghai Jiao Tong University Joint Institute, Shanghai Jiao Tong University, Shanghai, China in 2012 and 2017, respectively.

He is currently a postdoctoral researcher at Center for Ultra-Wide-Area Resilient Electric Energy Transmission Networks (CURENT), University of Tennessee, Knoxville, TN, USA. His research interests include optimization and energy management of microgrids and wireless power transfer systems, and



ultracapacitor hybrid energy storage systems, and on-line state-of-charge estimation algorithm for battery management systems.

Chen Zhao received the B.S. degree in electrical engineering and automation from East China University of Science and Technology, Shanghai, China, in 2011, and Ph.D. degree in electrical and computer engineering from University of Michigan-Shanghai Jiao Tong University Joint Institute, Shanghai Jiao Tong University, China, in 2016.

He is currently a systems engineer with United Automotive Electronic Systems Co., Ltd, Shanghai, China. His research interests include modeling and testing of lithium-ion batteries, control of battery-ultracapacitor hybrid energy storage systems, and on-line state-of-charge estimation algorithm for battery management systems.



Chengbin Ma (M'05-SM'18) received the B.S. (Hons.) degree in industrial automation from East China University of Science and Technology, Shanghai, China, in 1997, and the M.S. and Ph.D. degrees both in electrical engineering from The University of Tokyo, Tokyo, Japan, in 2001 and 2004, respectively.

He is currently an Associate Professor of electrical and computer engineering at University of Michigan-Shanghai Jiao Tong University Joint Institute, Shanghai Jiao Tong University, Shanghai, China. Between 2006 and 2008, he held a postdoctoral position with the Department of Mechanical and Aeronautical Engineering, University of California Davis, California, USA. From 2004 to 2006, he was an R&D researcher with Servo Laboratory, Fanuc Limited, Yamanashi, Japan. His research interests include energy management, megahertz wireless power transfer, dynamics and motion control, and wide applications in electronic devices, electric vehicles, microgrids and smart grids, etc.

Prof. Ma is an Associate Editor for the IEEE Transactions on Industrial Informatics.